Journal of
Medicinal Chemistry

Article

Heterodimeric analogues of the potent Y1R antagonist 1229U91, lacking one of the pharmacophoric C-terminal structures, retain potent Y1R affinity and show improved selectivity over Y4R.

Rachel Richardson, Marleen Groenen, Mengjie Liu, Simon J. Mountford, Stephen J. Briddon, Nicholas D. Holliday, and Philip E. Thompson

J. Med. Chem., **Just Accepted Manuscript** • DOI: 10.1021/acs.jmedchem.0c00027 • Publication Date (Web): 04 May 2020

Just Accepted

is published by the American Chemical Society. 1155 Sixteenth Street N.W., Washington, DC 20036

Heterodimeric analogues of the potent Y1R antagonist 1229U91, lacking one of the pharmacophoric C-terminal structures, retain potent Y1R affinity and show improved selectivity over Y4R.

Rachel R. Richardson[1,2], Marleen Groenen[2], Mengjie Liu[1], Simon J Mountford[1], Stephen J Briddon[2], Nicholas D Holliday[2], Philip E Thompson*[1]

[1]Medicinal Chemistry, Monash Institute of Pharmaceutical Sciences, 381 Royal Parade Parkville, VIC 3052, Australia

[2]Institute of Cell Signalling, School of Biomedical Sciences, University of Nottingham, Queen's Medical Centre, Nottingham, NG7 2UH, United Kingdom

***Author for correspondence: Prof. Philip E Thompson**

Medicinal Chemistry

Monash Institute of Pharmaceutical Sciences

381 Royal Parade

Parkville, VIC 3052

Australia

Tel: +61 3 9903 9672

Fax: +61 3 9903 9582

Email: philip.thompson@monash.edu

Abstract: The cyclic dimeric peptide, 1229U91 (GR231118) has an unusual structure and displays potent, insurmountable antagonism of the Y_1 receptor. To probe the structural basis for this activity we have prepared ring size variants and heterodimeric compounds, identifying the specific residues underpinning the mechanism of 1229U91 binding. The homodimeric structure was shown to be dispensible, with analogues lacking key pharmacophoric residues in one dimer arm retaining high antagonist affinity. Compounds **11d-h** also showed enhanced Y1R selectivity over Y4R compared to 1229U91.

Introduction

Neuropeptide Y (**1**, NPY) and its endocrine homologs peptide YY (PYY) and pancreatic polypeptide (PP) are 36-amino acid C-terminal amidated peptides with diverse physiological functions. NPY plays a key role as a central and peripheral sympathetic neurotransmitter, for example regulating feeding behavior, anxiety, and peripheral vasoconstriction.[1–3] As gastrointestinal hormones released following a meal, PYY and PP also provide important feedback mechanisms to regulate satiety via the hypothalamus, and gastrointestinal function.[2,4] In man, four $G_{i/o}$-protein coupled receptor (GPCR) subtypes (Y_1R, Y_2R, Y_4R and Y_5R) mediate the distinct actions of the NPY family[5,6] and considerable efforts have been made to develop subtype specific NPY receptor agonists and antagonists. For example, antagonists of the NPY / PYY selective Y_1R have been considered as potential therapeutics for obesity,[7] cancer,[8] hypertension[3] and gastrointestinal dysfunction.[4]

Both small-molecule and peptide-based antagonists have been described for the Y_1R. Small-molecule argininamide analogues of the NPY C-terminus, typified by compounds such as BIBO3226 (**2**) and UR-MK299 (**3**), are capable of sub-nanomolar affinity for the Y_1R.[9–13] The development of peptide ligands was initiated by the discovery that the C-terminal NPY decapeptide, Tyr-Ile-Asn-Leu-Ile-Tyr-Arg-Leu-Arg-Tyr-NH_2, possessed Y_1R antagonist properties,[14] with structure-activity relationship (SAR) studies confirming that, for the native NPY peptide, Arg^{33}, Arg^{35} and Tyr^{36} were essential for receptor binding and biological activity of this analogue. Based on this sequence, the subsequent peptide, BVD15 (**4**, BW1911U90; Ile-Asn-Pro-Ile-Tyr-Arg-Leu-Arg-Tyr-NH_2; Figure 1), showed increased Y_1R selectivity over the Y_2R by 40 fold,[14,15] and has since been used as the basis for DOTA, NOTA and 18F radiolabelled derivatives.[16–19]

The structure of BVD15 also underlay the development of the antiparallel homodimer 1229U91 (**5**, GR231118),[15] in which Glu^2 and Dap^4 substitutions allow formation of cross-linking lactam bridges between the two BVD15 monomers (Figure 1). 1229U91 is characterised by up to 100-fold higher apparent affinity and more potent competitive antagonism at Y_1R than BVD15, along with improvements in pharmacokinetic stability,[20,21] and has been a widely used tool to investigate the role

of the Y_1R in disease states.[22–26] Mechanistically, 1229U91 provides a stand out example of the unusual characteristic of several dimeric GPCR ligands to display much enhanced biological activity compared to their monomeric constituents. The significant increase in Y_1R affinity observed compared to BVD15 is insufficiently explained by simple consideration of the two-fold enhancement of the pharmacophore concentration due to bivalency. In some cases of dimeric ligand behaviour, the high potency of dimers has been attributed to interaction with oligomeric receptors.[27] In others, a bivalent ligand might increase the potential for receptor orthosteric site rebinding and slowing observed dissociation kinetics[28,29] by enhancing the local concentration of pharmacophore. Thirdly, the activity of dimers might be attributable to the capture of both intermediate and final binding poses as a ligand docks into the receptor binding site. Finally, it may simply be that certain dimers capture an extended receptor binding site by happenstance and the symmetry has no intrinsic special character.

Tyr-Pro-Ser-Lys-Pro-Asp-Asn-Pro-Gly-Glu-Asp-Ala-Pro-Ala-Glu-Asp-Leu-Ala-Arg-Tyr-Tyr-Ser-Ala-Leu-Arg-His-Tyr-Ile[28]-Asn-Leu-Ile[31]-Thr-Arg-Gln[34]-Arg-Tyr-NH_2

1, Neuropeptide Y

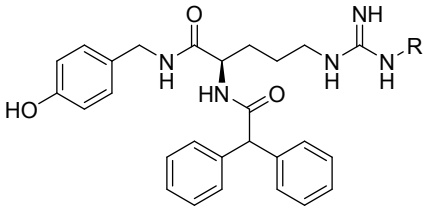

2, BIBP3226 R = H,
3, UR-MK299 R = $CONH(CH_2)_4NHCOCH_2CH_3$

Ile-Asn-Pro-Ile-Tyr-Arg-Leu-Arg-Tyr-NH_2

4, BVD15

Ile-Glu-Pro-Dap-Tyr-Arg-Leu-Arg-Tyr-NH_2

Ile-Glu-Pro-Dap-Tyr-Arg-Leu-Arg-Tyr-NH_2

5, 1229U91

Figure 1 - Y_1R receptor ligands.

A further characteristic of 1229U91 and its monomeric counterparts is the retention of appreciable affinity for the Y_4R. The Y_4R responds to PP and not NPY, but is most closely related to the Y_1R when considering Neuropeptide Y receptor family sequence homology.[30] Moreover 1229U91 shows low efficacy agonist, rather than antagonist activity at the Y_4 receptor,[20] and this agonism is also observed for BVD15[14,20,31] and its fluorescent derivative (sCy5)-[Lys^2Arg^4]-BVD15[32]. Understanding the SAR of 1229U91 at both receptors better may therefore provide a route to new Y_4R ligands, for which there is a limited pharmacological toolbox. For example, the state of play for Y_4 agonists, which are of

interest in promoting satiety[2], is represented by dimeric or modified C tail fragments of NPY such as BVD74-D,[33–35] or Tyr^{32}βCpe^{34}]-NPY$_{32-36}$,[36] with a single report of a small molecule allosteric modulator[37]. Y_4 antagonists to date have moderate affinity and tend to lack selectivity over the Y_1 receptor, with the exception of the dimeric argininamide compound, UR-MEK388, which was > 20 fold selective.[38,39] However the dual pharmacological profile displayed by 1229U91 (i.e. Y_1 antagonist / Y_4 agonist) might have favourable therapeutic advantages after optimisation, by mimicking both PP-mediated satiety and inhibiting the central appetite promoting effects of NPY.[2]

The synthesis of 1229U91 analogues for SAR studies is complicated by the risk of competing intramolecular lactam cyclisation and the cyclic monomer is a significant competing reaction.[15,40] In addition, the creation of heterodimers demands methods to unambiguously form appropriate interchain linkages. The early methods used to prepare 1229U91 utilised both Boc-based chemistry,[15] and Fmoc-based chemistry,[41] but are not well suited to preparing cyclic heterodimers.

We previously described the development of an unambiguous synthesis of cyclic dimers that avoids concomitant competing intramolecular cyclisation and allows the preparation of heterodimeric structures.[42] In an attempt to understand which of the above mechanisms governs the potent antagonism of Y1R by 1229U91, we have explored variation of ring cycle size within 1229U91, and conducted the first residue-by-residue interrogation within a single dimer arm. Our assessment of Y_1R antagonism and Y_4R agonism shows that the homodimer structure is not intrinsically important, but that the ring-proximal Tyr residue in the second arm makes a substantial contribution to Y_1R affinity through extended binding site contacts. Moreover, the 1229U91 ring structure plays a major role in dictating Y_1R potency and selectivity over its Y_4R homologue.

Results and Discussion

Chemistry

We pursued the solution phase formation of cyclic dimers via an orthogonal protection strategy described previously[42] to create a series of ring-size variant and alanine scanning modifications. The strategy is summarized for the ring size variants as shown in Scheme 1.[42]

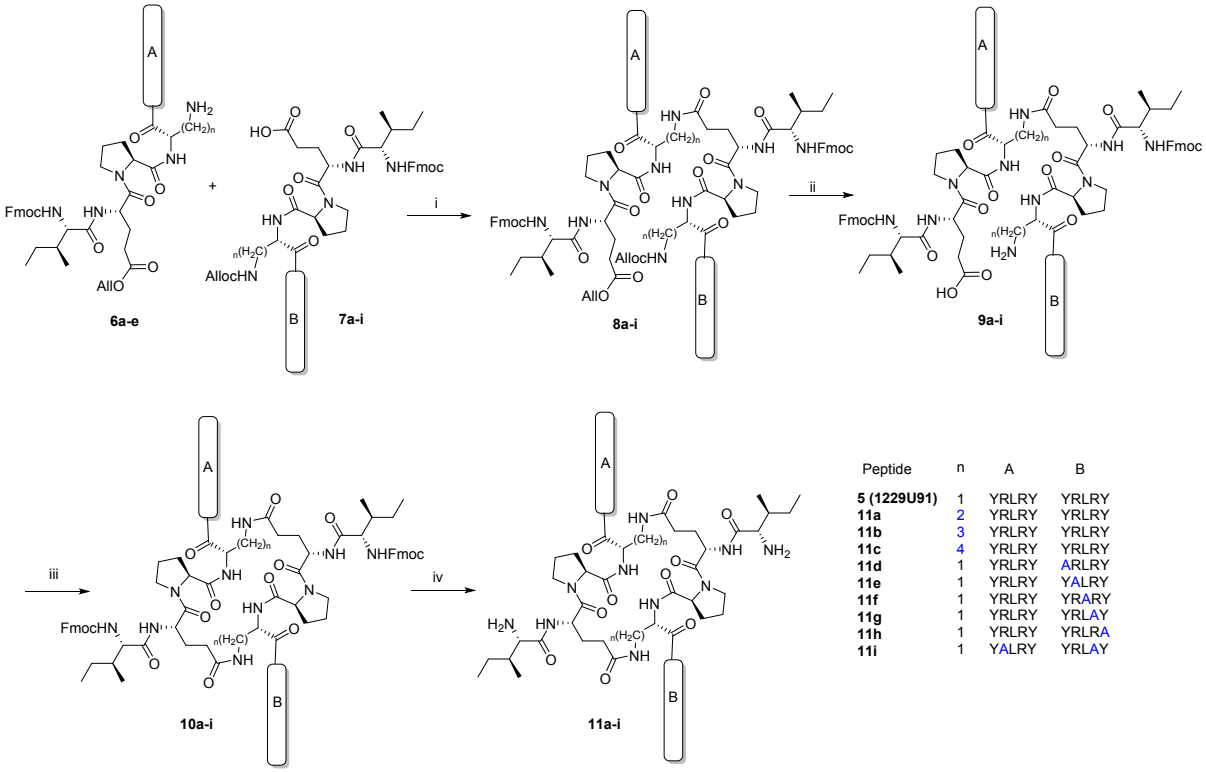

Peptide	n	A	B
5 (1229U91)	1	YRLRY	YRLRY
11a	2	YRLRY	YRLRY
11b	3	YRLRY	YRLRY
11c	4	YRLRY	YRLRY
11d	1	YRLRY	ARLRY
11e	1	YRLRY	YALRY
11f	1	YRLRY	YRARY
11g	1	YRLRY	YRLAY
11h	1	YRLRY	YRLRA
11i	1	YALRY	YRLAY

Scheme 1 – Synthesis of 1229U91 analogues. Reagents and conditions: (i) PyClock, TMP, DMF, RT, 12h. (ii) $Pd(PPh_3)_4$, $PhSiH_3$, DCM, MeOH,RT, 2h. (iii) PyClock, TMP, DMF, RT, 20h. (iv) piperidine, DMF, 0.5h.

This method was used to prepare homodimeric analogues **11a-c** with varied ring sizes and the heterodimeric alanine scan analogues **11d-i** as shown in Table 1. Full data are supplied in Supporting Information.

Firstly, two series of different partially protected peptides were prepared by conventional SPPS. In one series, a Glu(OAll) residue was included (**6a-e**) and in the other allyl carbamate (Alloc) protection was applied to the amine (Dap^4, Dab^4, Orn^4 and Lys^4) at position 4 (**7a-i**).

The two sequences were then linked by forming an intermolecular amide bridge between the unprotected Glu^2 and the amine containing residue at position 4 to give the branched intermediates (**8a-i**). The optimal conditions were that peptides **7** (1 equiv., 0.1M in DMF) were treated with PyClock (3 equiv.) followed by the addition of 2,4,6-trimethylpyridine (TMP,10 equiv.). Finally, peptide **6** (1 equiv.) was added and couplings were allowed to proceed for 12 h at room temperature, with additional PyClock (3 equiv.) added after 6h. The Alloc and OAll protecting groups of the cross linked peptides **8** were cleaved by treating the peptide with phenylsilane ($PhSiH_3$; 24 equiv.) and tetrakis(triphenylphosphine)palladium(0) ($Pd(PPh_3)_4$; 1 equiv; dissolved in 0.5 mL DCM) in MeOH under nitrogen for 2 h. These products **9** were then purified by RP-HPLC.

Cyclisation of the purified peptides was then achieved using PyClock (3 equiv.) and TMP (10 equiv.) in DMF (1 mg/ mL) with replenishment of these reagents twice across 20 h to give Fmoc-protected peptides **10.** These products were isolated by ether precipitation from a minimum volume of TFA, but not further purified. Final deprotection with piperidine in DMF gave the target peptides, **11a-i** which were purified by RP-HPLC. Overall yields between 1-4% were obtained, with the main losses due to close running impurities in RP-HPLC purification and in some cases incomplete cyclisation to form **10**.

Table 1 – Analytical data of Dimeric 1229U91 analogues.

Cpd #	Dimer sequence[a]	MW	ESI-MS[b]	RT[c] (min)	Yield[d] (mg)
5	Ile-Glu-Pro-**Dap**-Tyr-Arg-Leu-Arg-Tyr Ile-Glu-Pro-**Dap**-Tyr-Arg-Leu-Arg-Tyr	2351.3127	784.7803 $[M+3H]^{3+}$ 588.8385 $[M+4H]^{4+}$ 471.2727 $[M+5H]^{5+}$	5.6	20
11a	Ile-Glu-Pro-**Dab**-Tyr-Arg-Leu-Arg-Tyr Ile-Glu-Pro-**Dab**-Tyr-Arg-Leu-Arg-Tyr	2379.3440	794.1242 $[M+3H]^{3+}$ 595.8433 $[M+4H]^{4+}$ 476.8790 $[M+5H]^{5+}$	5.60	15
11b	Ile-Glu-Pro-**Orn**-Tyr-Arg-Leu-Arg-Tyr Ile-Glu-Pro-**Orn**-Tyr-Arg-Leu-Arg-Tyr	2407.3753	803.4675 $[M+3H]^{3+}$ 602.8546 $[M+4H]^{4+}$ 482.4848 $[M+5H]^{5+}$	5.64	3
11c	Ile-Glu-Pro-**Lys**-Tyr-Arg-Leu-Arg-Tyr Ile-Glu-Pro-**Lys**-Tyr-Arg-Leu-Arg-Tyr	2435.4066	812.8109 $[M+3H]^{3+}$ 609.8617 $[M+4H]^{4+}$ 488.0916 $[M+5H]^{5+}$	5.74	5
11d (Ala^5)	Ile-Glu-Pro-Dap-**Ala**-Arg-Leu-Arg-Tyr Ile-Glu-Pro-Dap-Tyr-Arg-Leu-Arg-Tyr	2259.2865	754.1053 $[M+3H]^{3+}$ 565.8317 $[M+4H]^{4+}$ 452.8674 $[M+5H]^{5+}$	5.47	5
11e (Ala^6)	Ile-Glu-Pro-Dap-Tyr-**Ala**-Leu-Arg-Tyr Ile-Glu-Pro-Dap-Tyr-Arg-Leu-Arg-Tyr	2266.2487	756.4266 $[M+3H]^{3+}$ 567.5722 $[M+4H]^{4+}$ 454.2599 $[M+5H]^{5+}$	6.03	18
11f (Ala^7)	Ile-Glu-Pro-Dap-Tyr-Arg-**Ala**-Arg-Tyr Ile-Glu-Pro-Dap-Tyr-Arg-Leu-Arg-Tyr	2309.2658	770.7611 $[M+3H]^{3+}$ 578.3266 $[M+4H]^{4+}$ 462.8634 $[M+5H]^{5+}$	5.26	26
11g (Ala^8)	Ile-Glu-Pro-Dap-Tyr-Arg-Leu-**Ala**-Tyr Ile-Glu-Pro-Dap-Tyr-Arg-Leu-Arg-Tyr	2266.2487	756.4254 $[M+3H]^{3+}$ 567.5721 $[M+4H]^{4+}$ 454.2595 $[M+5H]^{5+}$	5.78	20
11h (Ala^9)	Ile-Glu-Pro-Dap-Tyr-Arg-Leu-Arg-**Ala** Ile-Glu-Pro-Dap-Tyr-Arg-Leu-Arg-Tyr	2259.2865	754.1059 $[M+3H]^{3+}$ 565.8314 $[M+4H]^{4+}$ 754.1059 $[M+5H]^{5+}$	5.47	12
11i (Ala$^{6,8'}$)	Ile-Glu-Pro-Dap-Tyr-**Ala**-Leu-Arg-Tyr Ile-Glu-Pro-Dap-Tyr-Arg-Leu-**Ala**-Tyr	2181.1847	1091.6000 $[M+2H]^{2+}$ 728.0723 $[M+3H]^{3+}$ 546.3066 $[M+4H]^{4+}$	6.18	18

[a] Modification from **5** shown in bold, underlined. [b] HR-MS conditions as described in the Experimental section. [c] HPLC conditions: Zorbax Eclipse Plus C-18 Rapid Resolution 4.6 × 100 mm, 3.5 µm column (Agilent Technologies, Palo Alto, CA), 5-50% acetonitrile in 0.1% aq. TFA at 1ml/min over 8 minutes, 254nM. [d] Isolated yield from 0.3 mmol scale synthesis.

Pharmacology

Using the compounds described in Table 1, we assessed the influence of the various systematic structural changes on Y_1R affinity and antagonist behaviour and Y_4R affinity and agonist behaviour. Competition binding assays, using (sCy5)-[Lys^{2}Arg^4]-BVD15 as the fluorescent tracer, assessed compound affinity in Y_1-GFP or Y_4-GFP transfected HEK293T cells were performed.[32] Functional characterisation utilised NPY-induced recruitment of β-arrestin2 to the Y_1R or Y_4R as previously described.[32,34,43]

The ring size variants of 1229U91, compounds **11a**, **11b** and **11c** all showed high affinity for Y_1R with K_i values in the nanomolar range (Table 2), and were non-surmountable antagonists of NPY-induced β-arrestin2 recruitment as we have previously observed for other 1229U91 analogues (Figure 2A).[42] However, **11a**, **11b** and **11c** all showed 10 to 30-fold reduced Y_1R affinity compared to 1229U91 itself, with an equivalent decrease in their effects as antagonists (Figure 2B). The relatively reduced affinity of **11c,** compared to 1229U91 under these conditions is in contrast to our previously published data using a radioligand receptor binding assay against membrane homogenates from Y_2R / Y_4R knockout mice and recombinant cells.[42] As noted in our previous studies, better alignment of whole cell competition binding using fluorescent ligands and functional readouts are observed and to be expected, compared to radiolabeled agonist experiments in membrane homogenates.[32]

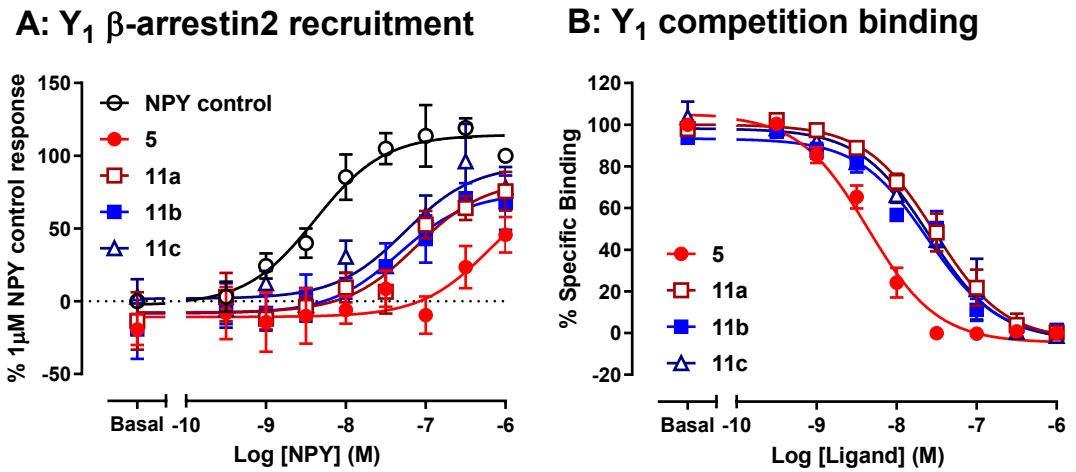

Figure 2 – Y_1R β-arrestin2 recruitment and competition binding by ring size variants – (A) Antagonism of NPY stimulated β-arrestin2 recruitment in Y_1 A2 cells by **5**, **11a-c** (30nM) compared to control. (B) Competition binding to determine ring variant peptide affinities, using 100 nM (sCy5)-[Lys^2Arg^4]-BVD15 as the fluorescent tracer in Y_1-GFP cells. Graphs were plotted from pooled data (n of 3 or more individual experiments) and represented as mean ± SEM in GraphPad Prism v7. Data in (A) were normalised to 1 μM NPY response, while (sCy5)-[Lys^2Arg^4]-BVD15 specific binding was defined by the presence or absence of 1 μM 1229U91 (analogue **5**).

Given 1229U91 (**5**) also binds the Y_4R, we counter-screened compounds **11a - 11c** in comparison to this peptide in Y_4R binding and β-arrestin2 recruitment studies. As we have previously reported, the potency of 1229U91 was 30-100 fold lower for the Y_4R compared to Y_1R in the β-arrestin2 assay.[32,42] 1229U91 displayed clear partial agonism compared to PP (Figure 3A). Changing the cyclic moiety in compounds **11a**, **11b** and **11c** had no significant impact on Y_4R affinity, or the potency of these compounds as partial agonists (Figure 3B). Indeed, the Lys derivative analogue **11c** demonstrated preserved Y_4R activity and an enhanced maximal response compared to 1229U91, accompanied by a loss of Y_1R:Y_4R selectivity compared to 1229U91 (Table 2). The activity of **11c** is similar, in these systems, to dimeric pentapeptide BVD74-D which represents the lead truncated synthetic ligand at the Y_4R.[32–34] Our data indicate that the larger ring size represented by the **11a** (Dab), **11b** (Orn) and **11c** (Lys) derivatives is better tolerated by the Y_4R than the Y_1R binding site, and further optimization of this aspect of the pharmacophore might increase Y_4R selectivity in future.

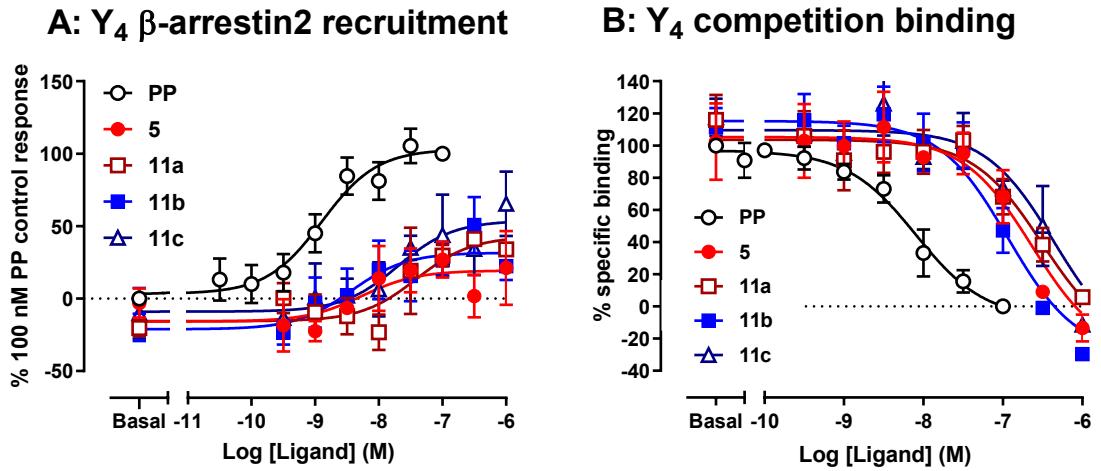

Figure 3 – Y_4R β-arrestin2 recruitment and competition binding by ring size variants – (A) Agonism of β-arrestin2 recruitment in Y_1 A2 cells by **PP**, **5**, **11a-c** compared to control. (B) Competition binding profile of ring variant dimers against 100 nM (sCy5)-[Lys^2Arg^4]-BVD15 in Y_4-GFP cells. Graphs were plotted from pooled data (n of 3 or more individual experiments) and represented as mean ± SEM in GraphPad Prism v7, normalised to 100 nM PP (A), or total specific binding in the absence of competing ligand (B). Non-specific binding of (sCy5)-[Lys^2Arg^4]-BVD15 was defined in the presence of 100 nM PP.

Table 2 – Summary of Y_1R and Y_4R pharmacology for 1229U91 ring size variant dimer peptides. Affinities were determined in Y_1 and Y_4 competition binding assays (pK_i) as indicated from Figure 2 and Figure 3. The agonist activities of the compounds in the Y_4 β-arrestin2 assay are presented as pEC_{50} and R_{max} (as percentage of 100 nM PP), with * $P < 0.05$, ** $P < 0.01$ compared to PP R_{max} (one way ANOVA followed by Dunnett's post test). All values are represented as mean ± SEM of at least 3 experiments. Finally the ratio of Y_4 / Y_1 mean K_i values is provided as an indication of selectivity.

Peptide	Y_1R	Y_4R			Y_4 / Y_1
	Binding	β-arrestin2		Binding	K_i
	pK_i	pEC_{50}	R_{max}	pK_i	selectivity
PP	-	7.90 ± 0.21	104.0 ± 5.7	8.19 ± 0.13	
5	8.99 ± 0.10	7.95 ± 0.25	21.8 ± 16.6**	7.05 ± 0.11	87
11a	8.09 ± 0.14	7.52 ± 0.23	43.8 ± 1.4*	6.81 ± 0.10	19
11b	7.89 ± 0.24	8.37 ± 0.43	33.0 ± 11.6*	7.20 ± 0.10	4.9
11c	7.60 ± 0.60	7.63 ± 0.31	56.4 ± 22.0	6.80 ± 0.18	6.3

Next, peptides **11d** – **11i** representing a C-terminal alanine scan of 1229U91 peptides were studied using the same assays. Previous data have clearly established the critical contributions of Arg^6, Arg^8 and Tyr^9 to Y_1R binding affinities of monomeric C-terminal peptides such as BVD15[14], and indeed full length NPY (Arg^{33}, Arg^{35} and Tyr^{36}).[44] Selective alanine substitution of these residues in one arm of the 1229U91 has potential to provide some insight into the molecular basis for the enhanced dimer affinity compared to the monomeric peptides. Mechanisms which consider receptor rebinding as a means to

slow ligand dissociation, or involve crosslinking orthosteric binding sites in a GPCR oligomer, predict that high affinity of both 1229U91 monomer arms for the target Y_1R binding site would be crucial. Single arm substitution of Arg^6, Arg^8 or Tyr^9 should demonstrate high impact on binding affinity in these scenarios.

In fact, the results do not support these hypotheses, showing that the "second C-terminus" has a distinct role in receptor binding at Y_1R and Y_4R. Of the 5 alanine-substituted peptides, the replacement of Tyr^5 by alanine, **11d** had the most profound effect with one order of magnitude reduction in the binding affinity compared to 1229U91 and a correspondingly reduced potency to antagonise NPY induced β-arrestin2 recruitment. (Figure 4). The replacement of Arg^6 by alanine, **11e,** led to a moderate 2-fold increase in K_i (Table 3), compared to 1229U91, and a similarly reduced antagonist action. The effects of Arg^6 substitution are most concisely explained as a simple loss of Y_1R binding site affinity from one arm of the bivalent ligand – and 2-fold reduction in the "effective" concentration of the pharmacophore[45].

Substitution of either Leu^7 (**11f**), Arg^8 (**11g**) or Tyr^9 (**11h**) by alanine had negligible effect, either on Y_1R affinity or functional antagonism in the β-arrestin2 assay, compared to 1229U91. The lack of effect of the other single arm alanine mutants in positions 7, 8 or 9 do not support an essential role of receptor dimers in generating their high Y_1R affinity. The continued overall importance of Arg^6 and Arg^8 in 1229U91 binding was demonstrated by combined substitution of alanine, replacing Arg^6 in one arm and Arg^8 in the other, **11i**. This double mutant showed much reduced affinity, by 100-fold compared to 1229U91, and no antagonism of NPY responses.

Collectively, these data provide significant evidence that following docking of the first arm of the 1229U91 dimer binding site, the second antiparallel peptide chain makes additional contacts with the Y_1R protein that extend the overall binding interface and enhance affinity. The implication is that the tyrosine 5 and tyrosine 5', proximal to the Dap-Glu lactam cycle, make distinct contacts that substantially explain the high affinity unique to the dimer compared to monomeric BVD15. This role of the linked tyrosine side chains, rather than the structural constraint or bulk provided by the ring itself,

is also consistent with our previous investigations of BVD15 monomeric analogues with rings at position 2-4 that do not, by themselves, lead to enhanced Y_1R affinity[46].

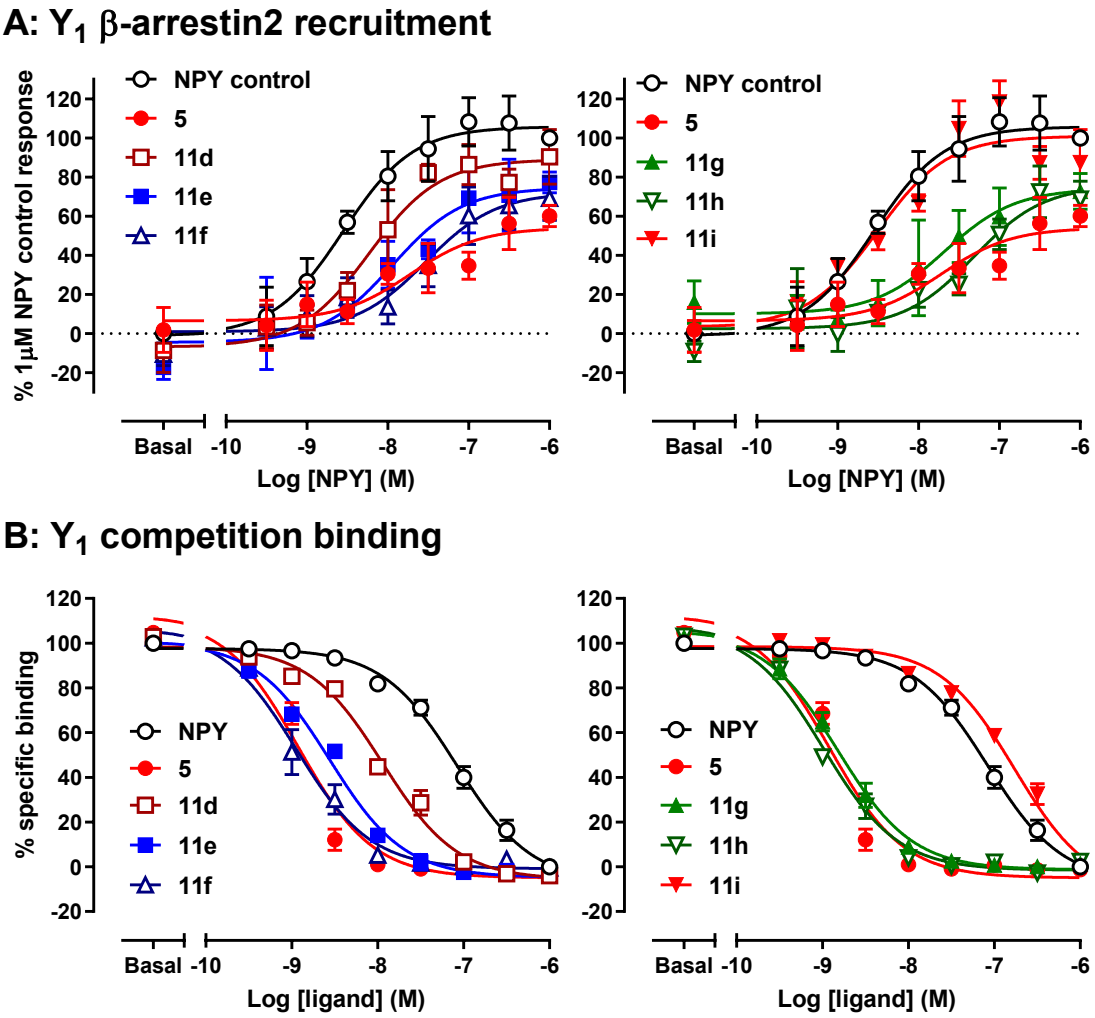

Figure 4 – Y_1R β-arrestin2 antagonism and competition binding by alanine substituted analogues – (A) Antagonism of NPY stimulated β-arrestin2 recruitment in Y_1 A2 cells by **5**, **11d-i** (3nM) compared to control. (B) Competition binding to determine **11d** – **11i** affinities in Y_1-GFP cells, using 100 nM (sCy5)-[Lys^{2}Arg^4]-BVD15 as the fluorescent tracer (NPY and **5** were used as control ligands). Non-specific binding was determined in the presence of 1 μM **5**. Graphs were plotted from pooled data as mean ± SEM (n of 3 or more individual experiments); data were normalised to the 1 μM NPY response (A), or total specific binding in the absence of competing ligand.

At the Y_4R, all alanine scan variants including **11d**, were characterized by a limited reduction in affinity compared to 1229U91 (consistent with simple loss of bivalency), but retained high potency and partial agonism in the β-arrestin2 assay (Figure 5A). For example, the Y_4R R_{max} value of **11g** (Ala^8), relative

to PP was not significantly different from 1229U91 (Table 3). Most notably, the effect of Tyr^5 substitution by alanine (**11e**) at the Y_1R is not preserved in the Y_4R binding site, and as for the ring variation highlights distinguishing SAR features between these two receptors. The dual substituted, $Ala^{6,8'}$-1229U91 **11i** could not fully displace the fluorescent ligand even at 10 μM and showed no agonist activity at concentrations up to 1 μM (Figure 5B).

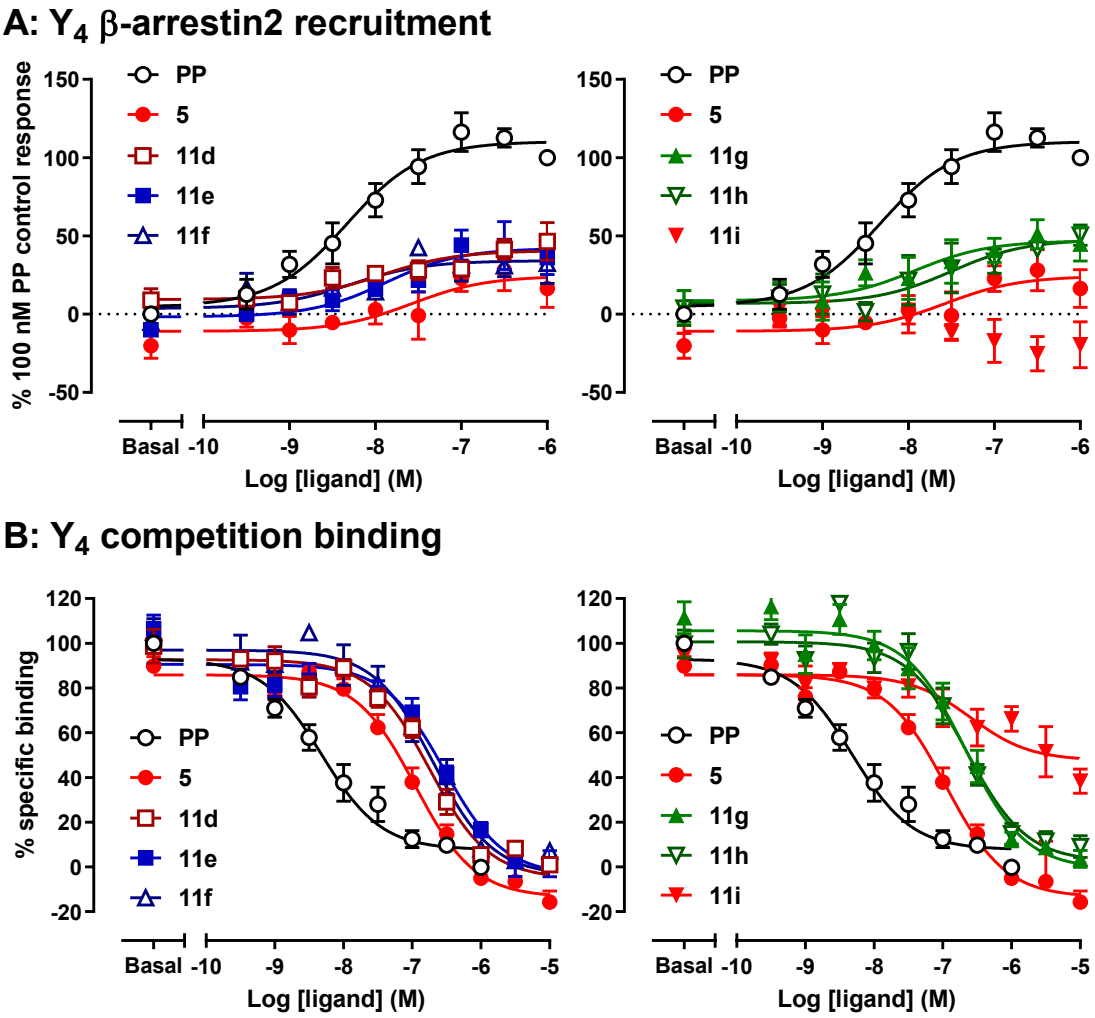

Figure 5 – Y_4R competition binding and β-arrestin2 recruitment by alanine sustituted 1229U91– (A) Agonism of β-arrestin2 recruitment in Y_1 A2 cells by **PP**, **5**, **11d-i** compared to control. (B) Competition binding using 100 nM (sCy5)-[Lys^2Arg^4]-BVD15 as the fluorescent tracer in Y_4-GFP cells. 100 nM PP defined non-specific binding. Data are pooled (mean ± SEM) from at least 3 experiments and normalised to 100 nM PP response (A) or specific binding in the absence of competing ligand (B).

A feature of the data set was the distinction between the activities of modified peptides at Y_1R compared to Y_4R. The Ki affinity ratios for competition binding suggest increased selectivity for alanine substituted dimers at the Y_1R compared to Y_4R (Table 3). In contrast, cycle variant 1229U91 analogues all displayed reduced selectivity between the two receptor subtypes (Table 2).

Table 3 – Summary of Y_1R and Y_4R pharmacology for 1229U91 alanine scan dimer peptides. Affinities were determined in competition binding assays (pK_i; Figure 4 and Figure 5). Agonist effects in the Y_4 β-arrestin2 assay are presented as pEC_{50} and R_{max} (as percentage of 100 nM PP). All values are represented as mean ± SEM of at least 3 experiments. Y_4 / Y_1 selectivity is indicated as the ratio of the mean K_i values.

Peptide	Y_1R	Y_4R			Y_4 / Y_1 K_i selectivity
	Binding	β-arrestin2		Binding	
	pK_i	pEC_{50}	R_{max}	pK_i	
NPY	7.78 ± 0.09	-	-	-	
PP	-	8.47 ± 0.27	112.1 ± 5.4	8.41 ± 0.18	
5	9.53 ± 0.04	7.43 ± 0.24	36.1 ± 5.6	7.38 ± 0.13	141
11d	8.63 ± 0.07	7.43 ± 0.81	52.3 ± 12.9	6.20 ± 0.08	269
11e	9.24 ± 0.03	8.12 ± 0.61	49.1 ± 13.0	6.61 ± 0.18	419
11f	9.56 ± 0.10	7.89 ± 0.20	48.2 ± 6.9	6.89 ± 0.14	427
11g	9.44 ± 0.03	8.29 ± 0.72	50.2 ± 8.0	6.77 ± 0.12	427
11h	9.59 ± 0.05	8.17 ± 0.81	55.2 ± 6.8	6.76 ± 0.11	676
11i	7.50 ± 0.06	-	-9.5 ± 18.0	6.04 ± 0.46	32

Discussion

1229U91 is an example of a dimeric, bivalent GPCR ligand which generates much higher affinity for the Y_1R than its constituent monomers, BVD15 and BVD15 derived analogues. The main aim of this

study was first to explore the contributions made by individual dimer arms, and the cyclic structure, within the 1229U91 derivative, to the high Y_1R binding affinity. Using a series of novel cyclic peptide analogues, we have been able to demonstrate that larger cycles within the 1229U91 dimer resulted in lower affinity at the Y_1R. This indicates that the nature of the cycle contributes to the high Y_1R affinity of 1229U91, with **5** (1229U91 itself) ring size being optimal. Using a series of novel single alanine substituted peptides we have determined that only $Tyr^{5'}$ in the second arm of 1229U91 is important in extending the dimer contact surface with the receptor and increasing affinity. In addition, we considered the impact of these analogue substitutions on the related Y_4R activity, and demonstrated that alterations in ring structure were better tolerated at this receptor binding site, preserving Y_4R agonism and led to analogues that were less selective at Y_1R:Y_4R. Equally $Tyr^{5'}$ in the second dimer arm was not a contributor to the observed Y_4R affinity of these analogues and substitution of the other residues with alanine had no effect. However, at least one intact arm was required in order to retain binding at the Y_4R, as shown with analogue **11i** ($Ala^{6,8'}$).

Increasing cycle size in 1229U91 dimeric peptides selectively reduced Y_1R binding affinity.

The novel synthesised 1229U91 dimer cyclic derivatives represented a systematic increase in the cyclic ring size at the heart of the dimer from Dap (1229U91; **5**) to Dab (**11a**) to Orn (**11b**) to Lys (**11c**). At the Y_1R these changes were accompanied by a progressive loss of binding affinity (up to 30 fold). There was an equivalent reduction in the ability of these ligands (at 30 nM) to act as antagonists of NPY-induced Y_1R β-arrestin2 recruitment, with a transition from non-surmountable to a more surmountable profile. This change in the nature of antagonism would be expected if, as assumed, the non-surmountable characteristics of 1229U91 in this assay derive from its high affinity and slowly reversible nature at the Y_1R.

In the original study reporting 1229U91,[15] a dimer derivative linked only by short Cys-Cys disulphide bonds at the 2,4 positions (383U91) displayed a modest 3 fold higher Y_1R affinity than BVD15,

compared to >100 fold for 1229U91 in this study. A second Dap dimer, linked only at position 4 (1120W91), without the cyclic constraint, had an intermediate effect on Y_1R affinity, increasing ~20 fold compared to BVD15. Together with the SAR of the novel cyclic analogues described here, it appears that the Dap^4 cycle in 1229U91 (**5**) represents the optimum cycle size for Y_1R activity. While larger cycles may sterically hinder analogue interaction to the Y_1R binding site, it may be that the increased flexibility is detrimental to affinity. The presence of cyclic Pro^3 in the macrocycle, adds to the rigidity and may provide an important feature for binding. Equally the Dap^4 cycle, replicated in the Dap linked dimers, but not in dimers with larger linkers or smaller linkers e.g. Cys-Cys bridges, may allow better positioning of residues in the second arm of the 1229U91 dimer for additional Y_1R contacts, thereby contributing to Y_1R high affinity.

Conversely for the Y_4R, the cyclic variants had no significant impact on the affinity of 1229U91 or its action as a partial agonist compared to PP in β-arrestin2 recruitment assays. Indeed, dimer derivatives with larger cycles, e.g. Lys^4 (**11c)**, demonstrated potential for a somewhat higher maximum response than 1229U91 itself, similar to the related dimeric peptide *R,R*-BVD-74D while still below that of PP itself.[34,35] Although some previous investigations have highlighted full agonist effects of 1229U91 compared to PP, for example in the inhibition of cAMP accumulation,[20] the efficacy of such ligands can be overestimated due to the signal amplification inherent in such assays.[47] With more limited receptor reserve, β-arrestin2 recruitment can provide a better guide to intrinsic ligand efficacy as changes in R_{max}. Nevertheless, given the possibility of ligand bias between signalling pathways,[47] it would be useful in future to confirm agonist properties of the Y_4R in G_i protein-coupled assay.

Overall the synthesised cyclic variants represent a class of compounds with reduced selectivity between the Y_1R and Y_4R, while retaining antagonist and agonist properties at each subtype, respectively. As Y_4R agonists, including PP and BVD74-D, have been shown to have a regulatory effect on food intake in mice,[48] and Y_1R antagonists such as 1229U91 and BIBO3304 have been shown to inhibit food intake in animal models[22,24,49] these less selective cyclic 1229U91 derivatives may represent potential for the

development of dual pharmacology ligands that could be desirable as starting points in anti-obesity agents.

The selective role of the second Tyr$^{5'}$ in the 1229U91 dimer peptide for Y_1R recognition

The alanine scan derivatives of 1229U91 (analogues **11d-11i**) were designed to explore the contribution of the second arm of the dimer to Y_1R binding affinity. Both monomer and dimer peptides are assumed to engage a similar core binding site to the NPY C-terminus on the Y_1R[14,44,50–54] and in particular, require key contacts for this affinity including; Arg^6, Arg^8, and the Tyr^9-amide. In the full length NPY peptide, single alanine substitution of the equivalent residues (Arg^{33}, Arg^{35} or Tyr^{36}) is sufficient for a dramatic loss in Y_1R binding affinity.[55] The heterodimeric 1229U91 analogues that were able to be constructed in which one peptide arm was preserved intact for engagement with the core Y_1R binding site, while investigating the effects on the second arm interactions and contribution to Y_1R binding affinity. Confirmation of the overall effects of Arg^6 and Arg^8 substitution in the dimeric ligands was achieved by their alanine substitution in separate arms of the **11i** analogue (Ala$^{6,8'}$) This analogue displayed substantial loss of both Y_1R affinity (100 fold) and antagonist action, predicted from the inability of either arm to engage with the core Y_1R binding site. Generally, the single alanine scan derivatives, at positions 6-9, showed only a modest reduction in Y_1R binding affinity, no more than would be predicted from the loss of bivalency and halving the effective concentration of the ligand required to engage the core Y_1R binding site. The exception was the Tyr$^{5'}$ substitution, analogue **11d**, in one arm of 1229U91, which resulted in a 10-fold loss of binding affinity suggesting that this residue in the second arm of a bound dimer plays a key role in Y_1R recognition. Our data therefore provide evidence to suggest that the high affinity of the 1229U91 dimer, in part, results from an extended Y_1R binding interface. In addition to the core C-terminus binding site, common to monomers and NPY itself, 1229U91 likely make use of cyclic peptide portion and the Tyr$^{5'}$ amino acid side chain in the second arm to make additional contacts with the Y_1R. In their original derivation of the BVD15 monomer peptide, the substitution of Thr^5, the native residue in NPY, for Tyr^5 was performed to increase affinity on the basis that this might replicate the necessary contribution of the amino terminal Tyr^1 of NPY to its high Y_1R

binding affinity.[14] Potentially the positioning of the second Tyr$^{5'}$ in 1229U91, combined with the optimal constraints of the Dap cycle, provides an optimal structure to replicate the NPY Tyr^{1} interaction in addition to its C-terminus contacts. The implication is that high affinity analogues equivalent to 1229U91 could be obtained without including a full dimer structure, preserving Tyr$^{5'}$, but not the remaining amino acids 6-9, in the second arm.

Previous studies have suggested that the Y_4R shares many of the same key residue interactions with ligands in its core binding site as the Y_1R. For example, modelling studies by Jois *et al.*, (2006) proposed that Arg^{6}, Arg^{8} and Tyr^{5} were involved in hydrogen bonding interactions between BVD15 at the both the Y_1R and the Y_4R.[56] However, these simulations were conducted in homology models and were not experimentally tested, e.g. by alanine scan peptides. Additionally, studies have confirmed direct ionic interactions of Arg^{35} in NPY and PP at Asp$^{6.59}$ in the Y_1R and Y_4R.[53] The loss of Y_4R agonism in analogue **11i** (Ala$^{6-8'}$), and lack of its full competition for binding at high concentrations, is consistent with these proposed interactions. However, in contrast to its effect in reducing Y_1R affinity, single alanine substitution of Tyr$^{5'}$ in the second arm of the peptide had no significant effect on Y_4R affinity or agonist properties, in common with the single alanine substitutions at other positions. This implies that the additional Y_1R interactions proposed for this second arm Tyr$^{5'}$ are not replicated in the Y_4R 1229U91 binding site. Given the hypothesis that this residue might mimic NPY Tyr^{1} in Y_1R binding, it is worth noting that this Tyr residue is not preserved in the human PP sequence, but is an alanine in PP, and is therefore unlikely to be recognised by the Y_4R. Future modelling studies should enable greater molecular understanding of the differences in Y_1R and Y_4R interaction implied by the Ala^{5} and cyclic variant 1229U91 analogues.

Conclusions

In this work we have characterised a series of cyclic 1229U91 dimeric derived peptides at the Y_1R and the Y_4R in order to investigate the role of the cyclic structure in receptor recognition and selectivity. Our studies have shown that the cyclic moiety within the dimer compounds plays a role in Y_1R recognition, with the original Dap^{4} based cycles in 1229U91 being optimal. In contrast, larger cycles

may have a limited positive impact on agonist activity at Y_4R. In addition to the role of the cyclic moiety, we have successfully investigated the role of the single dimer arm residues in Y_1R and Y_4R activity, through the generation and characterisation of 1229U91 dimer alanine substitution derivatives. These compounds revealed an important role for $Tyr^{5'}$ in the second arm of 1229U91 in contributing to high Y_1R, but not Y_4R affinity. This suggests that $Tyr^{5'}$ interacts with the receptor at a different site from its position on the first arm, mimicking the NPY C-terminus binding mode, potentially replicating the role of NPY Tyr^1. Overall this identifies a structural basis for explaining, in part, the higher affinity of dimeric versus monomeric peptide derivatives for the Y_1R. With the advent of the first Y receptor crystal structure,[12] molecular modelling studies could be undertaken to support the hypotheses implied by our SARs, and to identify new Y receptor contact residues which could then be explored by receptor mutagenesis. The data in this study provides evidence for a 1229U91 binding interactions that does not rely on the homodimeric structure per se, but operates as a high affinity cyclic peptide that presents the C-terminal pentapeptide in canonical fashion to NPY, but gains its high affinity from unique behaviour of the macrocycle and the tyrosine residue of the second arm. The refinement of the SAR provides a roadmap for the development of novel heterodimeric or non-dimeric structures that have advantageous pharmacological properties.

Experimental Section

Peptide chemistry

All solvents were obtained from Merck and Sigma Aldrich and were of analytical grade (Castle Hill, NSW, Australia). All Fmoc-protected amino acids were purchased from ChemImpex (Wood Dale, IL, USA) along with Rink amide resin, HCTU and PyClock. All commercially obtained chemicals were used without further purification. LCMS vials and silicone liners were purchased from Adelab Scientific (Thebarton, SA, Australia). All other plastic consumables were purchased from GreinerBio (Kremsmunster, Austria) unless otherwise stated.

RP-HPLC was performed on a Phenomenex Luna C-8 column (100Å, 10µm, 250×50.0mm) utilising a Waters 600 semi-preparative HPLC incorporating a Waters 486 UV detector. Eluting profile was a linear gradient of 0-80 % acetonitrile in water over 60 min at a flow rate of 15 ml / min.

ESI-MS analysis (Method A) using a Shimadzu LCMS2020 instrument, incorporating a Phenomenex Luna C-8 column (100 Å, 3 µm, 100×2.00 mm). Eluting profile was a linear gradient of 100 % water for 4 min, followed by 0-80 % acetonitrile in water over 15 min and isocratic 80% acetonitrile for 1 min, at a flow rate of 0.2 ml / min.

Analytical RP-HPLC (Method B) was conducted on an Agilent Infinity 1260 system fitted with Zorbax Eclipse Plus C-18 Rapid Resolution 4.6 × 100 mm, 3.5 µm column (Agilent Technologies, Palo Alto, CA) using a binary solvent system (solvent A: 0.1% TFA, 99.9% H2O; solvent B: 0.1% TFA, 99.9% acetonitrile (ACN), with ultraviolet (UV) detection at 254 nm. The method used a linear gradient elution profile of 5-50% solvent B over 8 min at a flow rate of 1 mL/min. All peptides assayed were of > 95% purity.

HRMS analyses were performed on an Agilent 6224 time-of-flight (TOF) Mass Spectrometer coupled to an Agilent 1290 Infinity liquid chromatographer (LC/MS) (Agilent, Palo Alto, CA). All data were acquired and reference mass corrected via a dual-spray electrospray ionisation (ESI) source. Each scan or data point on the Total Ion Chromatogram (TIC) is an average of 13,700 transients, producing one spectrum every second. Mass spectra were created by averaging the scans across each peak and background subtracting against the first 10 seconds of the TIC. The acquisition was performed using the Agilent Mass Hunter Data Acquisition software version B.05.00 Build 5.0.5042.2 and analysis were performed using Mass Hunter Qualitative Analysis version B.05.00 Build 5.0.519.13. MS conditions were: Drying gas flow: 11 L/min; Nebuliser: 45 psi; Drying gas temperature: 325 °C; Capillary Voltage (Vcap): 4000 V; Fragmentor: 160 V; Skimmer: 65 V; OCT RFV: 750 V; Scan range acquired: 100–1500 *m/z*; Internal Reference ions: Positive Ion Mode = *m/z* = 121.050873 and 922.009798.

Solid phase synthesis methods

All linear peptides were synthesised following Fmoc-based solid phase peptide synthesis (SPPS) strategies using a PS3 automated peptide synthesiser (Protein Technologies Inc, Tucson, AZ, USA). Peptides were synthesized on Rink amide resin on a 0.3mmol scale. Deprotections were carried out using 20 % piperidine in DMF (2 x 5 min) to remove Fmoc protecting groups. Couplings were carried out with 3-fold molar excess of protected amino acids and coupling reagent, O-(1*H*-6-chlorobenzotriazole-1-yl)-1,1,3,3-tetramethyluronium hexafluorophosphate) (HCTU). After coupling of the final amino acid the resin was washed with DMF (3 x 5 mL), MeOH (3 x 5 mL) and Et_2O (4 x 5 mL) and dried.

The resin-bound linear peptide was treated with a solution of triisopropylsilane (TIPS; 5 %) and 1,3-dimethoxybenzene (DMB; 2.5 %) in trifluoroacetic acid (TFA), and then shaken for 2-3 h at RT. The resin was then filtered and washed with TFA (3 mL) and the filtrate collected. The filtrate was concentrated under nitrogen (30 min) and the peptide was precipitated out in ice cold Et_2O (up to 30 mL). The suspension was sonicated (1 min) and cooled at 0 °C (30 min), then centrifuged (3000 rpm; 5 min). The supernatant was discarded, the residue was then washed with ether and centrifuged again. The precipitate was allowed to air dry and was then re-suspended in 50:50 acetonitrile (MeCN):H_2O. A small sample was then analysed by liquid chromatography- mass spectrometry (LCMS) to confirm the desired peptide product, before lyophilisation to yield the linear peptides.

Preparation of linear peptides

All linear peptides were synthesised following Fmoc-based solid phase peptide synthesis (SPPS) strategies using a PS3 automated peptide synthesiser (Protein Technologies Inc, Tucson, AZ, USA). Peptides were synthesized on Rink amide resin on a 0.3mmol scale. Deprotections were carried out using 20 % piperidine in DMF (2 x 5 min) to remove Fmoc protecting groups. Couplings were carried out with 3-fold molar excess of protected amino acids and coupling reagent, O-(1*H*-6-chlorobenzotriazole-1-yl)-1,1,3,3-tetramethyluronium hexafluorophosphate) (HCTU). After coupling of the final amino acid the resin was washed with DMF (3 x 5 mL), MeOH (3 x 5 mL) and Et_2O (4 x 5 mL) and dried.

The resin-bound linear peptide was treated with a solution of triisopropylsilane (TIPS; 5 %) and 1,3-dimethoxybenzene (DMB; 2.5 %) in trifluoroacetic acid (TFA), and then shaken for 2-3 h at RT. The resin was then filtered and washed with TFA (3 mL) and the filtrate collected. The filtrate was concentrated under nitrogen (30 min) and the peptide was precipitated out in ice cold Et_2O (up to 30 mL). The suspension was sonicated (1 min) and cooled at 0 °C (30 min), then centrifuged (3000 rpm; 5 min). The supernatant was discarded, the residue was then washed with ether and centrifuged again. The precipitate was allowed to air dry and was then re-suspended in 50:50 acetonitrile (MeCN):H2O. A small sample was then analysed by liquid chromatography- mass spectrometry (LCMS) to confirm the desired peptide product, before lyophilisation and purification by RP-HPLC to yield the linear peptides.

1229U91 (**5**) was prepared as previously described.[42]

White solid (15 mg).

RT (A) 7.59 min (B) 5.6 min

HRMS: $C_{110}H_{170}N_{34}O_{24}$ 2351.323 (Found) 2351.3127 (Calc.) m/z 784.7803 $[M+3H]^{3+}$, 588.8385 $[M+4H]^{4+}$, 471.2727 $[M+5H]^{5+}$.

Fmoc-Ile-Glu(OAll)-Pro-Dap-Tyr-Arg-Leu-Arg-Tyr-NH_2 (**6a**)

White solid (197 mg, 99 % purity).

ESI-MS: m/z 729.4 $[M+2H]^{2+}$ 486.6 $[M+3H]^{3+}$; RT (A) 9.95 min.

Fmoc-Ile-Glu(OAll)-Pro-Dab-Tyr-Arg-Leu-Arg-Tyr-NH_2 (**6b**)

White solid (98 mg, 99 % purity)

ESI-MS: m/z 735.9 $[M+2H]^{2+}$ 490.9 $[M+3H]^{3+}$; RT (A) 9.99 min.

Fmoc-Ile-Glu(OAll)-Pro-Orn-Tyr-Arg-Leu-Arg-Tyr-NH_2 (**6c**)

White solid (160 mg, 98 % purity).

ESI-MS: m/z 743.4 $[M+2H]^{2+}$ 495.9 $[M+3H]^{3+}$; RT (A) 10.05 min,

Fmoc-Ile-Glu(OAll)-Pro-Lys-Tyr-Arg-Leu-Arg-Tyr-NH_2 (**6d**)

White solid (136 mg, 98 % purity).

ESI-MS: m/z 750.4 $[M+2H]^{2+}$ 500.6 $[M+3H]^{3+}$; RT (A) 14.45 min

Fmoc-Ile-Glu(OAll)-Pro-Dap-Tyr-Ala-Leu-Arg-Tyr-NH_2 (**6e**)

White solid (117 mg, 99 % purity).

ESI-MS: m/z 686.8 $[M+2H]^{2+}$; RT (A) 10.64 min.

Fmoc-Ile-Glu-Pro-Dap(Alloc)-Tyr-Arg-Leu-Arg-Tyr-NH_2 (**7a**)

White solid (74 mg, 99 % purity).

ESI-MS: m/z 751.4 $[M+2H]^{2+}$; RT (A) 10.30 min

Fmoc-Ile-Glu-Pro-Dab(Alloc)-Tyr-Arg-Leu-Arg-Tyr-NH_2 (**7b**)

White solid (105 mg, 99 % purity).

ESI-MS: m/z 758.4 $[M+2H]^{2+}$; RT (A) 10.32 min.

Fmoc-Ile-Glu-Pro-Orn(Alloc)-Tyr-Arg-Leu-Arg-Tyr-NH_2 (**7c)**

White solid (130 mg, 99 % purity). ESI-MS: m/z 764.9 $[M+2H]^{2+}$; RT (A) 10.35 min,

Fmoc-Ile-Glu-Pro-Lys(Alloc)-Tyr-Arg-Leu-Arg-Tyr-NH_2 (**7d**)

White solid (83 mg, 99 % purity).

ESI-MS: m/z 772.4 $[M+2H]^{2+}$; RT (A) 15.04 min.

Fmoc-Ile-Glu-Pro-Dap(Alloc)-Ala-Arg-Leu-Arg-Tyr-NH_2 (**7e**)

White solid (142 mg, 99 % purity).

ESI-MS: m/z 705.32 $[M+2H]^{2+}$; RT (A) 10.40 min,

Fmoc-Ile-Glu-Pro-Dap(Alloc)-Tyr-Ala-Leu-Arg-Tyr-NH_2 (**7f**)

White solid (116 mg, >99 % purity).

ESI-MS: m/z 708.8 $[M+2H]^{2+}$; RT (A) 11.18 min.

Fmoc-Ile-Glu-Pro-Dap(Alloc)-Tyr-Arg-Ala-Arg-Tyr-NH_2 (**7g**)

White solid (175 mg, 99 % purity).

ESI-MS: m/z 730.3 $[M+2H]^{2+}$; RT (A) 10.24 min

Fmoc-Ile-Glu-Pro-Dap(Alloc)-Tyr-Arg-Leu-Ala-Tyr-NH_2 (**7h**)

White solid (132 mg, >99 % purity).

ESI-MS: m/z 708.81 $[M+2H]^{2+}$; RT (A) 10.98 min

Fmoc-Ile-Glu-Pro-Dap(Alloc)-Tyr-Arg-Leu-Arg-Ala-NH_2 (**7i**)

White solid (158 mg, 98 % purity).

ESI-MS: m/z 705.37 $[M+2H]^{2+}$; RT (A) 10.37 min.

Solution phase amide bond formation conditions

Peptides **6** (1 equiv) were suspended in DMF (0.1M) containing 6-chloro-benzotriazole-1-yloxy-tris-pyrrolidinophosphonium hexafluorophosphate (Pyclock; 3 equiv.) and 2,4,6-trimethypyridine (TMP; 10 equiv.) and then **7** (1 equiv.) was added. The reaction was stirred for 12 h at RT, with additional PyClock (3 equiv.) added after 6h then concentrated in vacuo. The residue was re-suspended in TFA (0.5 mL) and **8** was precipitated out in ice cold Et_2O as described above. A sample was analysed by LCMS to confirm the desired coupling had occurred. The product was not further purified but reacted as follows.

OAll/Alloc side chain deprotection: The peptides **8** were treated with phenylsilane (PhSiH3; 24 equiv.) and tetrakis(triphenylphosphine)palladium(0) (Pd(PPh3)4; 1 equiv; dissolved in 0.5 mL DCM) in MeOH. The reaction was left to stir under nitrogen for 2 h. The reaction mixture was concentrated under vacuum and the product was washed with DCM (2-3 mL; x 1). The reaction mixture was then concentrated under vacuum again and resuspended in TFA (0.5 mL). The peptide was precipitated out in ice cold Et_2O. A sample was analysed by LCMS to confirm the desired peptide product. The crude peptide was purified using RP-HPLC to give peptide analogues, **9.**

9a

White solid (97 mg, 99 % purity)

ESI-MS: m/z 948.8 $[M+3H]^{3+}$, 711.9 $[M+4H]^{4+}$; RT (A) 10.07 min.

9b

White solid (111 mg, 97 % purity).

ESI-MS: m/z 958.1 $[M+3H]^{3+}$, 718.9 $[M+4H]^{4+}$; RT (A) 10.05 min.

9c

White solid (65 mg, 99 % purity)

ESI-MS: m/z 967.5 $[M+3H]^{3+}$, 725.9 $[M+4H]^{4+}$; RT (A) 10.01 min.

9d

ESI-MS: m/z 908.7 $[M+3H]^{3+}$,947.1 $[M+TFA+3H]^{3+}$, 681.8 $[M+4H]^{4+}$; RT (A) 10.10 min.

9e

White solid (31 mg, 98 % purity).

ESI-MS: m/z 1366.1 $[M+2H]^{2+}$, 911.1 $[M+3H]^{3+}$, 683.6 $[M+4H]^{4+}$; RT (A)10.38 min.

9f

White solid (45 mg, 99 % purity).

ESI-MS: m/z 1366.1 $[M+2H]^{2+}$, 911.1 $[M+3H]^{3+}$, 963.4 $[M+TFA+3H]^{3+}$, 683.6 $[M+4H]^{4+}$; RT (A) 10.09 min.

9g

White solid (34 mg, 99 % purity).

ESI-MS: m/z 1366.1 $[M+2H]^{2+}$,911.1 $[M+3H]^{3+}$,683.6 $[M+4H]^{4+}$; RT (A) 10.39 min.

9h

White solid (30 mg, 99 % purity).

ESI-MS: m/z 946.7 $[M+TFA+3H]^{3+}$,908.7 $[M+3H]^{3+}$, 681.8 $[M+4H]^{4+}$; RT (A) 10.11 min.

9i

White solid (39 mg, 97 % purity).

ESI-MS: m/z 1323.5 $[M+2H]^{2+}$, 882.7 $[M+3H]^{3+}$; RT (A) 10.81 min.

Final cyclisation and Fmoc deprotection

Peptides **9** were suspended in DMF containing 6-chloro-benzotriazole-1-yloxy-tris-pyrrolidinophosphonium hexafluorophosphate (Pyclock; 3 equiv.) and 2,4,6-trimethypyridine (TMP; 10 equiv.). The reaction was stirred for 12 h at RT, then concentrated in vacuo. The residue was re-suspended in TFA (0.5 mL) and the peptide **10** was precipitated out in ice cold Et_2O as described above. The residue was treated with 20 % piperidine in DMF, shaken for 30 min at RT. It was then immediately concentrated in vacuo. The lyophilised product was re-suspended in TFA (0.5 mL) and the peptide was precipitated out in ice cold Et_2O as previously described. The crude peptide was purified using RP-HPLC to give the products **5** and **11a-i**.

[$Dab^{3,3'}$]1229U91 (**11a**)

White solid (15 mg)

ESI-MS: m/z 1305.4 $[M+2TFA+2H]^{2+}$, 832.6 $[M+TFA+3H]^{3+}$, 794.6 $[M+3H]^{3+}$ and 596.2 $[M+4H]^{4+}$.

HRMS: $C_{112}H_{174}N_{34}O_{24}$ 2379.3546 (Found) 2379.344 (Calc.); m/z 794.1242 $[M+3H]^{3+}$, 595.8433 $[M+4H]^{4+}$, 476.8790 $[M+5H]^{5+}$

RT (A) 7.59 min, (B) 5.6 min

[Orn$^{3,3'}$]1229U91 (**11b**)

white solid (3 mg,

ESI-MS: m/z 1319.5 $[M+2TFA+2H]^{2+}$, 842.0 $[M+TFA+3H]^{3+}$, 804.0 $[M+3H]^{3+}$ and 603.2 $[M+4H]^{4+}$.

HRMS: $C_{114}H_{178}N_{34}O_{24}$ 2407.3873 (Found) 2407.3753 (Calc.) m/z 794.1242 $[M+3H]^{3+}$, 595.8433 $[M+4H]^{4+}$, 476.8790 $[M+5H]^{5+}$.

RT (A) 7.64 min, (B) 5.64 min.

[Lys$^{3,3'}$]1229U91 (**11c)**

White solid (5 mg)

ESI-MS: m/z 1333.2 $[M+2TFA+2H]^{2+}$, 851.1 $[M+TFA+3H]^{3+}$, 813.1 $[M+3H]^{3+}$ and 610.1 $[M+4H]^{4+}$.

HRMS: $C_{116}H_{182}N_{34}O_{24}$ 2435.4173 (Found) 2435.4066 (Calc.). m/z 812.8109 $[M+3H]^{3+}$, 609.8617 $[M+4H]^{4+}$, 488.0916 $[M+5H]^{5+}$

RT (A) 7.71 min, (B) 5.74 min

[Ala^{5}]1229U91 (**11d**)

White solid (5 mg)

ESI-MS: m/z 1245.5 $[M+2TFA+2H]^{2+}$, 792.7 $[M+TFA+3H]^{3+}$, 754.7 $[M+3H]^{3+}$ and 566.2 $[M+4H]^{4+}$.

HRMS: $C_{104}H_{166}N_{34}O_{23}$ 2259.2987 (Found) 2259.2865 (Calc.); m/z 754.1053 $[M+3H]^{3+}$, 565.8317 $[M+4H]^{4+}$, 452.8674 $[M+5H]^{5+}$.

RT (A) 7.44 min, (B) 5.47 min

[Ala^{6}]1229U91 (**11e**)

White solid, (18 mg)

ESI-MS: m/z 757.0 $[M+3H]^{3+}$. RT 7.84 min, as a white solid (18 mg, 99 % purity).

HRMS: $C_{107}H_{163}N_{31}O_{24}$ 2266.2582 (Found) 2266.2487 (Calc.); m/z 756.4266 $[M+3H]^{3+}$, 567.5722 $[M+4H]^{4+}$, 454.2599 $[M+5H]^{5+}$.

RT (A) 7.84 min, (B) 6.03 min.

[Ala^{7}]1229U91 (**11f**)

White solid (26 mg)

ESI-MS: m/z 1270.5 $[M+2TFA+2H]^{2+}$, 809.3 $[M+TFA+3H]^{3+}$, 771.3 $[M+3H]^{3+}$ and 578.8 $[M+4H]^{4+}$.

HRMS: $C_{107}H_{164}N_{34}O_{24}$ 2309.2754 (Found) 2309.2658 (Calc.); m/z 770.7611 $[M+3H]^{3+}$, 578.3266 $[M+4H]^{4+}$, 462.8634 $[M+5H]^{5+}$.

RT (A) 7.28 min, (B) 5.26 min.

[Ala^{8}]1229U91 (**11g**)

White solid (20 mg)

ESI-MS: m/z 757.0 $[M+3H]^{3+}$. RT 7.70 min, as a , 99 % purity).

HRMS: $C_{107}H_{163}N_{31}O_{24}$ 2309.2754 (Found) 2309.2658 (Calc.); m/z 756.4254 $[M+3H]^{3+}$, 567.5721 $[M+4H]^{4+}$, 454.2595 $[M+5H]^{5+}$.

RT (A) 7.70 min, (B) 5.78 min.

[Ala^{9}]1229U91 (**11h**)

White solid (12 mg)

ESI-MS: m/z 1245.5 $[M+2TFA+2H]^{2+}$, 792.7 $[M+TFA+3H]^{3+}$, 754.77 $[M+3H]^{3+}$ and 566.3 $[M+4H]^{4+}$.

HRMS: $C_{104}H_{166}N_{34}O_{23}$ 2259.2973 (Found) 2259.2865 (Calc.); 754.1059 $[M+3H]^{3+}$, 565.8314 $[M+4H]^{4+}$, 754.1059 $[M+5H]^{5+}$.

RT (A) 7.78 min, (B) 5.47 min.

[Ala$^{6,8'}$]1229U91 (**11i**)

White solid (18 mg)

ESI-MS: m/z 1092.5 $[M+2H]^{2+}$ and 728.7 $[M+3H]^{3+}$

HRMS: $C_{104}H_{156}N_{28}O_{24}$ 2181.194 (Found) 2181.1847 (Calc.) m/z 1091.6000 $[M+2H]^{2+}$, 728.0723 $[M+3H]^{3+}$, 546.3066 $[M+4H]^{4+}$

RT (A) 8.38 min, (B) 6.18 min.

Receptor Binding Methods

Cell culture

HEK293T and 293TR cells (Invitrogen) were cultured in Dulbecco's modified Eagle's medium (DMEM, Sigma-Aldrich) supplemented with 10 % foetal bovine serum, and passaged when confluent by trypsinisation (0.25 % w/v in Versene). Mixed population 293TR cell lines inducibly expressing Y receptors tagged with C-terminal GFP, and dual stable HEK293 cell lines expressing Y receptor-Yc and β-arrestin2-Yn (where Yc, and Yn are complementary fragments of YFP), and have both been described elsewhere.[43,57]

Functional analysis of Y receptor - β-arrestin2 recruitment

This analysis used bimolecular fluorescence complementation (BiFC) based detection of Y receptor – β-arrestin2 association, as described previously.[43,57] Y_1R β-arrestin2 or Y_4R β-arrestin2 BiFC cell lines were seeded at 40 000 cells / well onto poly-D-lysine coated 96 well black-bottomed plates (655090, Greiner Bio-One, Gloucester, U.K.), and experiments were performed once cells reached confluence at 24 h. Medium was replaced with DMEM / 0.1 % bovine serum albumin (BSA), and if appropriate cells were pre-treated for 30 min at 37°C with 1229U91 analogues (3-30 nM). Human NPY, human PP (Bachem, St. Helens, U.K.) and peptide analogues were then added for 60 min (10^{-11} M - 3 x 10^{-6} M, triplicate wells). Incubations were terminated by fixation with 3 % paraformaldehyde in phosphate buffered saline (PBS, 15 min at 21°C), the cells were washed once with PBS and the cell nuclei were stained for 15 min with the permeable dye H33342 (2 μg ml^{-1} in PBS, Sigma). H33342 was then removed by a final PBS wash. Images (4 central sites / well) were acquired automatically on an IX Ultra confocal plate reader (Molecular Devices, Sunnyvale CA, U.S.A.), equipped with a Plan Fluor 40x NA 0.6 extra-long working distance objective and 405 nm / 488 nm laser lines for H33342 and GFP excitation respectively.

An automated granularity algorithm (MetaXpress 5.1, Molecular Devices) identified internal fluorescent compartments within these images of at least 3 μm diameter (range set to 3 – 18 μm). For

each experiment, granules were classified on the basis of intensity thresholds which were set manually with reference to the negative (vehicle) or positive (1 μM NPY or 100 nM PP) plate controls. The response for each data point was quantified as mean granule average intensity / cell, from assessment of 12 images (4 sites / well in triplicate), normalised to the reference agonist response. Concentration response curves were fitted to the individual experiments by non-linear least squares regression (GraphPad Prism) to obtain agonist potency (pEC_{50}) and maximum response (R_{max}) estimates. Functional estimates of Y_1 antagonist affinity were not obtained from NPY concentration response curve shifts due to the insurmountable nature of the antagonism. Data are pooled (mean ± SEM) from at least 3 experiments.

(sCy5)-[Lys^{2}Arg^4]-BVD15 competition binding assays

293TR Y_1-GFP or Y_4-GFP cells were seeded at 20 000 cells / well in poly-D-lysine coated 96 well imaging plates (Greiner 655090), treated with 1 μg ml^{-1} tetracycline for 18 – 21 h and then used in experiments at confluence. As required, cells were labelled with membrane impermeant SNAP surface Alexa Fluor (AF) 488 in complete DMEM for 30 min (37 °C, 5 % CO2; .2 μM). Cells were washed in HEPES-buffered saline solution (HBSS) including 0.1 % BSA. Cells were the incubated in HEPES containing H33342 (2 μg ml^{-1}) and varying concentrations of competitor ligands (10^{-10} M to 10^{-6} M) for 5 min, prior to the addition of (sCy5)-[Lys^{2}Arg^4]-BVD15 at a final concentration of 100 nM. Incubations were continued for 30 min at 37°C, after which the media was replaced with HBSS / 0.1 % BSA (to remove free fluorescent compound). The cells were immediately imaged (2 sites / well) on a Molecular Devices IX Ultra confocal plate reader (Molecular Devices, Sunnyvale CA, U.S.A.) equipped with a Plan Fluor 40x NA 0.6 extra-long working distance objective and 405 nm / 488 nm and 633 nm laser lines for H33342, SNAP AF488 and (sCy5)-[Lys^{2}Arg^4]-BVD15 excitation, respectively. Read time was less than 10 min, and repeated "total" wells at the end of the read confirmed stable binding of the fluorescent ligand over this period.

Bound ligand fluorescence was quantified by granularity analysis (2-3 μm diameter granules; count per cell using MetaXpress), and normalised to positive (totals 100 %) and negative (0 %, presence of 1 μM

NPY or 100 nM PP) controls. IC_{50} values were then determined using GraphPad Prism, and converted to K_i using the Cheng-Prusoff correction (based on pre-determined (sCy5)-[Lys^2Arg^4]-BVD15 K_d values of 30 nM and 300 nM for the Y_1R and Y_4R, respectively).[32] Data are pooled (mean ± SEM) from at least 3 experiments.

Author Information: philip.thompson@monash.edu

ORCID ID: 0000-0002-5910-7625

Acknowledgements

Rachel Richardson was supported by a Joint University of Nottingham-Monash University Post Graduate Award scholarship.

Supporting Information

The Supporting Information is available free of charge on the ACS Publications website at DOI:.

SMILES codes and RP-HPLC chromatograms of peptides.

Abbreviations

NPY, Neuropeptide Y; pancreatic polypeptide (PP); peptide YY (PYY); YFP, yellow fluorescent protein;

References

(1) Wettstein, J. G.; Earley, B.; Junien, J. L. Central Nervous System Pharmacology of Neuropeptide Y. *Pharmacol. Ther.* **1995**, *65* (3), 397–414.

(2) Brothers, S. P.; Wahlestedt, C. Therapeutic Potential of Neuropeptide y (NPY) Receptor Ligands. *EMBO Mol. Med.* **2010**, *2* (11), 429–439. https://doi.org/10.1002/emmm.201000100.

(3) Tan, C. M. J.; Green, P.; Tapoulal, N.; Lewandowski, A. J.; Leeson, P.; Herring, N. The Role of Neuropeptide Y in Cardiovascular Health and Disease. *Front. Physiol.* **2018**, *9*, 1281. https://doi.org/10.3389/fphys.2018.01281.

(4) Cox, H. M. Neuroendocrine Peptide Mechanisms Controlling Intestinal Epithelial Function. *Curr. Opin. Pharmacol.* **2016**, *31*, 50–56. https://doi.org/10.1016/j.coph.2016.08.010.

(5) Blomqvist, A. G.; Herzog, H. Y-Receptor Subtypes--How Many More? *Trends Neurosci.* **1997**, *20* (7), 294–298.

(6) Cabrele, C.; Beck-Sickinger, A. G. Molecular Characterization of the Ligand-Receptor Interaction of the Neuropeptide Y Family. *J. Pept. Sci.* **2000**, *6* (3), 97–122. https://doi.org/10.1002/(SICI)1099-1387(200003)6:3<97::AID-PSC236>3.0.CO;2-E.

(7) Sato, N.; Ogino, Y.; Mashiko, S.; Ando, M. Modulation of Neuropeptide Y Receptors for the Treatment of Obesity. *Expert Opin. Ther. Pat.* **2009**, *19* (10), 1401–1415. https://doi.org/10.1517/13543770903251722.

(8) Ruscica, M.; Dozio, E.; Motta, M.; Magni, P. Relevance of the Neuropeptide Y System in the Biology of Cancer Progression. *Curr. Top. Med. Chem.* **2007**, *7* (17), 1682–1691.

(9) Doods, H. N.; Wieland, H. A.; Engel, W.; Eberlein, W.; Willim, K.; Entzeroth, M.; Wienen, W.; Rudolf, K. : : BIBP 3226, the first selective neuropeptide Y1 receptor antagonistReview of Its Pharmacological Properties 1. *Regulatory Peptides* **1996**, *65*, 71–77.

(10) Wieland, H. A.; Engel, W.; Eberlein, W.; Rudolf, K.; Doods, H. N. Subtype Selectivity of the Novel Nonpeptide Neuropeptide Y Y1 Receptor Antagonist BIBO 3304 and Its Effect on Feeding in Rodents. *Br. J. Pharmacol.* **1998**, *125* (3), 549–555. https://doi.org/10.1038/sj.bjp.0702084.

(11) Keller, M.; Schindler, L.; Bernhardt, G.; Buschauer, A. Toward Labeled Argininamide-Type NPY Y1 Receptor Antagonists: Identification of a Favorable Propionylation Site in BIBO3304. *Arch. Pharm. (Weinheim).* **2015**, *348* (6), 390–398. https://doi.org/10.1002/ardp.201400427.

(12) Yang, Z.; Han, S.; Keller, M.; Kaiser, A.; Bender, B. J.; Bosse, M.; Burkert, K.; Kögler, L. M.;

Wifling, D.; Bernhardt, G.; Plank, N.; Littmann, T.; Schmidt, P.; Yi, C.; Li, B.; Ye, S.; Zhang, R.; Xu, B.; Larhammar, D.; Stevens, R. C.; Huster, D.; Meiler, J.; Zhao, Q.; Beck-Sickinger, A. G.; Buschauer, A.; Wu, B. Structural Basis of Ligand Binding Modes at the Neuropeptide YY1 Receptor. *Nature* **2018**, *556* (7702), 520–524. https://doi.org/10.1038/s41586-018-0046-x.

(13) Dumont, Y.; St-Pierre, J. A.; Quirion, R. Comparative Autoradiographic Distribution of Neuropeptide Y Y1 Receptors Visualized with the Y1 Receptor Agonist [125I][Leu31,Pro34]PYY and the Non-Peptide Antagonist [3H]BIBP3226. *Neuroreport* **1996**, *7* (4), 901–904.

(14) Leban, J. J.; Heyer, D.; Landavazo, A.; Matthews, J.; Aulabaugh, A.; Daniels, A. J. Novel Modified Carboxy Terminal Fragments of Neuropeptide Y with High Affinity for Y2-Type Receptors and Potent Functional Antagonism at a Y1-Type Receptor. *J. Med. Chem.* **1995**, *38* (7), 1150–1157.

(15) Daniels, A. J.; Matthews, J. E.; Slepetis, R. J.; Jansen, M.; Viveros, O. H.; Tadepalli, A.; Harrington, W.; Heyer, D.; Landavazo, A.; Leban, J. J.; Spaltenstein, A. High-Affinity Neuropeptide Y Receptor Antagonists. *Proc. Natl. Acad. Sci. U. S. A.* **1995**, *92* (20), 9067–9071.

(16) Guérin, B.; Dumulon-perreault, V.; Tremblay, M.; Ait-mohand, S.; Fournier, P.; Dubuc, C.; Authier, S.; Bénard, F. Bioorganic & Medicinal Chemistry Letters [Lys (DOTA) 4] BVD15 , a Novel and Potent Neuropeptide Y Analog Designed for Y 1 Receptor-Targeted Breast Tumor Imaging. *Bioorg. Med. Chem. Lett.* **2010**, *20* (3), 950–953. https://doi.org/10.1016/j.bmcl.2009.12.068.

(17) Pourghiasian, M.; Inkster, J.; Hundal, N.; Mesak, F.; Guerin, B.; Ait-Mohand, S.; Ruth, T.; Adam, M.; Lin, K.-S.; Benard, F. 18F-BVD-15 for NPY Y1 Receptor Imaging in Breast Cancer and Neuroblastoma Models by PET. *J. Nucl. Med.* **2011**, *52* (supplement 1), 1682–1682.

(18) Guérin, B.; Ait-Mohand, S.; Tremblay, M. C.; Dumulon-Perreault, V.; Fournier, P.; Bénard, F. Total Solid-Phase Synthesis of NOTA-Functionalized Peptides for PET Imaging. *Org. Lett.* **2010**, *12* (2), 280–283. https://doi.org/10.1021/ol902601x.

(19) Liu, M.; Mountford, S. J.; Zhang, L.; Lee, I.-C.; Herzog, H.; Thompson, P. E. Synthesis of BVD15 Peptide Analogues as Models for Radioligands in Tumour Imaging. *Int. J. Pept. Res. Ther.* **2013**, *19* (1), 33–41. https://doi.org/10.1007/s10989-012-9330-z.

(20) Parker, E. M.; Babij, C. K.; Balasubramaniam, A.; Burrier, R. E.; Guzzi, M.; Hamud, F.; Mukhopadhyay, G.; Rudinski, M. S.; Tao, Z.; Tice, M.; Xia, L.; Mullins, D. E.; Salisbury, B. G. GR231118 (1229U91) and Other Analogues of the C-Terminus of Neuropeptide Y Are Potent Neuropeptide Y Y1 Receptor Antagonists and Neuropeptide Y Y4 Receptor Agonists. *Eur. J. Pharmacol.* **1998**, *349* (1), 97–105.

(21) Hegde, S. S.; Bonhaus, D. W.; Stanley, W.; Eglen, R. M.; Moy, T. M.; Loeb, M.; Shetty, S. G.; DeSouza, A.; Krstenansky, J. Pharmacological Evaluation of 1229U91, a Novel High-Affinity and Selective Neuropeptide Y-Y1 Receptor Antagonist. *J. Pharmacol. Exp. Ther.* **1995**, *275* (3), 1261–1266.

(22) Veyrat-Durebex, C.; Quirion, R.; Ferland, G.; Dumont, Y.; Gaudreau, P. Aging and Long-Term Caloric Restriction Regulate Neuropeptide Y Receptor Subtype Densities in the Rat Brain. *Neuropeptides* **2013**, *47* (3), 163–169. https://doi.org/10.1016/j.npep.2013.01.001.

(23) Kermani, M.; Eliassi, A. Gastric Acid Secretion Induced by Paraventricular Nucleus Microinjection of Orexin A Is Mediated through Activation of Neuropeptide Yergic System. *Neuroscience* **2012**, *226*, 81–88. https://doi.org/10.1016/j.neuroscience.2012.08.052.

(24) Zheng, H.; Townsend, R. L.; Shin, A. C.; Patterson, L. M.; Phifer, C. B.; Berthoud, H. R. High-Fat Intake Induced by Mu-Opioid Activation of the Nucleus Accumbens Is Inhibited by Y1R-Blockade and MC3/4R-Stimulation. *Brain Res.* **2010**, *1350*, 131–138. https://doi.org/10.1016/j.brainres.2010.03.061.

(25) Nedungadi, T. P.; Briski, K. P. Effects of Intracerebroventricular Administration of the NPY-Y1 Receptor Antagonist, 1229U91, on Hyperphagic and Glycemic Responses to Acute and Chronic Intermediate Insulin-Induced Hypoglycemia in Female Rats. *Regul. Pept.* **2010**, *159* (1–3), 14–18. https://doi.org/10.1016/j.regpep.2009.07.006.

(26) Dark, J.; Pelz, K. M. NPY Y1 Receptor Antagonist Prevents NPY-Induced Torpor-like Hypothermia in Cold-Acclimated Siberian Hamsters. *Am. J. Physiol. Regul. Integr. Comp. Physiol.* **2008**, *294* (1), R236-245. https://doi.org/10.1152/ajpregu.00587.2007.

(27) Hubner, H.; Schellhorn, T.; Gienger, M.; Schaab, C.; Kaindl, J.; Leeb, L.; Clark, T.; Moller, D.; Gmeiner, P. Structure-Guided Development of Heterodimer-Selective GPCR Ligands. *Nat. Commun.* **2016**, *7*, 1–12. https://doi.org/10.1038/ncomms12298.

(28) Vauquelin, G.; Charlton, S. J. Long-Lasting Target Binding and Rebinding as Mechanisms to Prolong in Vivo Drug Action. *Br. J. Pharmacol.* **2010**, *161* (3), 488–508. https://doi.org/10.1111/j.1476-5381.2010.00936.x.

(29) Vauquelin, G. Effects of Target Binding Kinetics on in Vivo Drug Efficacy: Koff , Kon and Rebinding. *Br. J. Pharmacol.* **2016**, *173* (15), 2319–2334. https://doi.org/10.1111/bph.13504.

(30) Larhammar, D.; Salaneck, E. Molecular Evolution of NPY Receptor Subtypes. *Neuropeptides* **2004**, *38* (4), 141–151. https://doi.org/10.1016/j.npep.2004.06.002.

(31) Balasubramaniam, A.; Dhawan, V. C.; Mullins, D. E.; Chance, W. T.; Sheriff, S.; Guzzi, M.; Prabhakaran, M.; Parker, E. M. Highly Selective and Potent Neuropeptide Y (NPY) Y1 Receptor Antagonists Based on [Pro(30), Tyr(32), Leu(34)]NPY(28-36)-NH2 (BW1911U90). *J. Med. Chem.* **2001**, *44* (10), 1479–1482.

(32) Liu, M.; Richardson, R. R.; Mountford, S. J.; Zhang, L.; Tempone, M. H.; Herzog, H.; Holliday, N. D.; Thompson, P. E. Identification of a Cyanine-Dye Labeled Peptidic Ligand for Y1R and Y4R, Based upon the Neuropeptide Y C-Terminal Analogue, BVD-15. *Bioconjug. Chem.* **2016**, *27* (9), 2166–2175. https://doi.org/10.1021/acs.bioconjchem.6b00376.

(33) Kuhn, K. K.; Ertl, T.; Dukorn, S.; Keller, M.; Bernhardt, G.; Reiser, O.; Buschauer, A. High Affinity Agonists of the Neuropeptide Y (NPY) Y4 Receptor Derived from the C-Terminal Pentapeptide of Human Pancreatic Polypeptide (HPP): Synthesis, Stereochemical Discrimination, and Radiolabeling. *J. Med. Chem.* **2016**, *59* (13), 6045–6058. https://doi.org/10.1021/acs.jmedchem.6b00309.

(34) Liu, M.; Mountford, S. J.; Richardson, R. R.; Groenen, M.; Holliday, N. D.; Thompson, P. E. Optically Pure, Structural, and Fluorescent Analogues of a Dimeric Y4 Receptor Agonist Derived by an Olefin Metathesis Approach. *J. Med. Chem.* **2016**, *59* (13), 6059–6069. https://doi.org/10.1021/acs.jmedchem.6b00310.

(35) Mullins, D. E.; Slack, K.; Dhawan, V. C.; Guzzi, M.; Parker, E. M.; Lin, S.; Tao, Z.; Zhai, W.; Knittel, J. J.; Herzog, H.; Balasubramaniam, A. Neuropeptide Y (NPY) Y 4 Receptor Selective Agonists Based on NPY(32−36): Development of an Anorectic Y 4 Receptor Selective Agonist with Picomolar Affinity . *J. Med. Chem.* **2006**, *49* (8), 2661–2665. https://doi.org/10.1021/jm050907d.

(36) Berlicki, L.; Kaske, M.; Gutierrez-Abad, R.; Bernhardt, G.; Illa, O.; Ortuno, R. M.; Cabrele, C.; Buschauer, A.; Reiser, O. Replacement of Thr32 and Gln34 in the C-Terminal Neuropeptide Y Fragment 25-36 by Cis-Cyclobutane and Cis-Cyclopentane Beta-Amino Acids Shifts Selectivity toward the Y(4) Receptor. *J. Med. Chem.* **2013**, *56* (21), 8422–8431. https://doi.org/10.1021/jm4008505.

(37) Schubert, M.; Stichel, J.; Du, Y.; Tough, I. R.; Sliwoski, G.; Meiler, J.; Cox, H. M.; Weaver, C. D.; Beck-Sickinger, A. G. Identification and Characterization of the First Selective Y4 Receptor Positive Allosteric Modulator. *J. Med. Chem.* **2017**, *60* (17), 7605–7612. https://doi.org/10.1021/acs.jmedchem.7b00976.

(38) Kuhn, K. K.; Littmann, T.; Dukorn, S.; Tanaka, M.; Keller, M.; Ozawa, T.; Bernhardt, G.; Buschauer, A. In Search of NPY Y4R Antagonists: Incorporation of Carbamoylated Arginine, Aza-Amino Acids, or d -Amino Acids into Oligopeptides Derived from the C-Termini of the

Endogenous Agonists. *ACS Omega* **2017**, *2* (7), 3616–3631. https://doi.org/10.1021/acsomega.7b00451.

(39) Keller, M.; Kaske, M.; Holzammer, T.; Bernhardt, G.; Buschauer, A. Dimeric Argininamide-Type Neuropeptide y Receptor Antagonists: Chiral Discrimination between Y1 and Y4 Receptors. *Bioorganic Med. Chem.* **2013**, *21* (21), 6303–6322. https://doi.org/10.1016/j.bmc.2013.08.065.

(40) Balasubramaniam, A. Neuropeptide Y Family of Hormones: Receptor Subtypes and Antagonists. *Peptides* **1997**, *18* (3), 445–457. https://doi.org/10.1016/S0196-9781(96)00347-6.

(41) Lew, M. J.; Murphy, R.; Angus, J. A. Synthesis and Characterization of a Selective Peptide Antagonist of Neuropeptide Y Vascular Postsynaptic Receptors. *Br. J. Pharmacol.* **1996**, *117* (8), 1768–1772.

(42) Mountford, S. J.; Liu, M.; Zhang, L.; Groenen, M.; Herzog, H.; Holliday, N. D.; Thompson, P. E. Synthetic Routes to the Neuropeptide Y Y1 Receptor Antagonist 1229U91 and Related Analogues for SAR Studies and Cell-Based Imaging. *Org. Biomol. Chem.* **2014**, *12* (20), 3271–3281. https://doi.org/10.1039/c4ob00176a.

(43) Kilpatrick, L. E.; Briddon, S. J.; Hill, S. J.; Holliday, N. D. Quantitative Analysis of Neuropeptide y Receptor Association with β-Arrestin2 Measured by Bimolecular Fluorescence Complementation. *Br. J. Pharmacol.* **2010**, *160* (4), 892–906. https://doi.org/10.1111/j.1476-5381.2010.00676.x.

(44) Beck-Sickinger, A. G.; Wieland, H. A.; Wittneben, H.; Willim, K. D.; Rudolf, K.; Jung, G. Complete L-Alanine Scan of Neuropeptide Y Reveals Ligands Binding to Y1 and Y2 Receptors with Distinguished Conformations. *Eur. J. Biochem.* **1994**, *225* (3), 947–958. https://doi.org/10.1111/j.1432-1033.1994.0947b.x.

(45) Lane, J. R.; Sexton, P. M.; Christopoulos, A. Bridging the Gap: Bitopic Ligands of G-Protein-Coupled Receptors. *Trends Pharmacol. Sci.* **2013**, *34* (1), 59–66.

https://doi.org/10.1016/j.tips.2012.10.003.

(46) Northfield, S. E.; Mountford, S. J.; Wielens, J.; Liu, M.; Zhang, L.; Herzog, H.; Holliday, N. D.; Scanlon, M. J.; Parker, M. W.; Chalmers, D. K.; Thompson, P. E. Propargyloxyproline Regio- and Stereoisomers for Click-Conjugation of Peptides: Synthesis and Application in Linear and Cyclic Peptides. *Aust. J. Chem.* **2015**, *68* (9), 1365–1372. https://doi.org/10.1071/CH15146.

(47) Stott, L. A.; Hall, D. A.; Holliday, N. D. Unravelling Intrinsic Efficacy and Ligand Bias at G Protein Coupled Receptors: A Practical Guide to Assessing Functional Data. *Biochem. Pharmacol.* **2016**, *101*, 1–12. https://doi.org/10.1016/j.bcp.2015.10.011.

(48) Li, J. B.; Asakawa, A.; Terashi, M.; Cheng, K.; Chaolu, H.; Zoshiki, T.; Ushikai, M.; Sheriff, S.; Balasubramaniam, A.; Inui, A. Regulatory Effects of Y4 Receptor Agonist (BVD-74D) on Food Intake. *Peptides* **2010**, *31* (9), 1706–1710. https://doi.org/10.1016/j.peptides.2010.06.011.

(49) Yulyaningsih, E.; Zhang, L.; Herzog, H.; Sainsbury, A. NPY Receptors as Potential Targets for Anti-Obesity Drug Development. *Br. J. Pharmacol.* **2011**, *163* (6), 1170–1202. https://doi.org/10.1111/j.1476-5381.2011.01363.x.

(50) Fuhlendorff, J.; Gether, U.; Aakerlund, L.; Langeland-Johansen, N.; Thøgersen, H.; Melberg, S. G.; Olsen, U. B.; Thastrup, O.; Schwartz, T. W. [Leu31, Pro34]Neuropeptide Y: A Specific Y1 Receptor Agonist. *Proc. Natl. Acad. Sci. U. S. A.* **1990**, *87* (1), 182–186.

(51) Gehlert, D. R.; Schober, D. A.; Gackenheimer, S. L.; Beavers, L.; Gadski, R.; Lundell, I.; Larhammar, D. [125I]Leu31, Pro34-PYY Is a High Affinity Radioligand for Rat PP1/Y4 and Y1 Receptors: Evidence for Heterogeneity in Pancreatic Polypeptide Receptors. *Peptides* **1997**, *18* (3), 397–401. https://doi.org/10.1016/S0196-9781(96)00346-4.

(52) Kaiser, A.; Müller, P.; Zellmann, T.; Scheidt, H. A.; Thomas, L.; Bosse, M.; Meier, R.; Meiler, J.; Huster, D.; Beck-Sickinger, A. G.; Schmidt, P. Unwinding of the C-Terminal Residues of

Neuropeptide Y Is Critical for Y_2 Receptor Binding and Activation. *Angew. Chem. Int. Ed. Engl.* **2015**, *54* (25), 7446–7449. https://doi.org/10.1002/anie.201411688.

(53) Merten, N.; Lindner, D.; Rabe, N.; Römpler, H.; Mörl, K.; Schöneberg, T.; Beck-Sickinger, A. G. Receptor Subtype-Specific Docking of Asp6.59 with C-Terminal Arginine Residues in Y Receptor Ligands. *J. Biol. Chem.* **2007**, *282* (10), 7543–7551. https://doi.org/10.1074/jbc.M608902200.

(54) Pedragosa-Badia, X.; Sliwoski, G. R.; Nguyen, E. D.; Lindner, D.; Stichel, J.; Kaufmann, K. W.; Meiler, J.; Beck-Sickinger, A. G. Pancreatic Polypeptide Is Recognized by Two Hydrophobic Domains of the Human Y4 Receptor Binding Pocket. *J. Biol. Chem.* **2014**, *289* (9), 5846–5859. https://doi.org/10.1074/jbc.M113.502021.

(55) Beck-Sickinger, A. G.; Jung, G. Structure - Activity Relationships of Neuropeptide Y Analogues with Respect to Y1 and Y2 Receptors. *Biopolymers* **1995**, *37* (2), 123–142. https://doi.org/10.1002/bip.360370207.

(56) Jois, S. D. S.; Nagarajarao, L. M.; Prabhakaran, M.; Balasubramaniam, A. Modeling of Neuropeptide Receptors Y1, Y4, Y5, and Docking Studies with Neuropeptide Antagonist. *J. Biomol. Struct. Dyn.* **2006**, *23* (5), 497–508.

(57) Kilpatrick, L. E.; Briddon, S. J.; Holliday, N. D. Fluorescence Correlation Spectroscopy, Combined with Bimolecular Fluorescence Complementation, Reveals the Effects of β-Arrestin Complexes and Endocytic Targeting on the Membrane Mobility of Neuropeptide Y Receptors. *Biochim. Biophys. Acta - Mol. Cell Res.* **2012**, *1823* (6), 1068–1081. https://doi.org/10.1016/j.bbamcr.2012.03.002.

Table of Contents Graphic